RAPID COMMUNICATION

# Gas treatment protection of metallic lithium anode*

Wen-jun Li(李文俊)[1,2], Quan Li(李泉)[1,2], Jie Huang(黄杰)[1,2], Jia-yue Peng(彭佳悦)[1,2], Geng Chu(褚赓)[1,2], Ya-xiang Lu(陆雅翔)[1], Jie-yun Zheng(郑杰允)[1], and Hong Li(李泓)[1,†]

[1] *Beijing National Laboratory for Condensed Matter Physics, Institute of Physics, Chinese Academy of Sciences, Beijing* 100190, *China*
[2] *University of Chinese Academy of Sciences, Beijing* 100049, *China*

(Received 20 May 2017; revised manuscript received 31 May 2017; published online 10 July 2017)

The effects of different coating layers on lithium metal anode formed by reacting with different controlled atmospheres (argon, $CO_2$–$O_2$(2:1), $N_2$, and $CO_2$–$O_2$–$N_2$(2:1:3)) have been investigated. The obtained XRD, second ion mass spectroscopy (SIMS), and scanning probe microscope (SPM) results demonstrate the formation of coating layers composed of $Li_2CO_3$, $Li_3N$, and the mixture of them on lithium tablets, respectively. The Li/Li symmetrical cell and Li/S cell are assembled to prove the advantages of the protected lithium tablet on electrochemical performance. The comparison of SEM and SIMS characterizations before/after cycles clarifies that an SEI-like composition formed on the lithium tablets could modulate the interfacial stabilization between the lithium foil and the ether electrolyte.

**Keywords:** gas treatment, lithium metal anode, lithium ion battery, lithium protection

**PACS:** 82.47.Aa, 65.40.gk, 82.45.Fk **DOI:** 10.1088/1674-1056/26/8/088202

## 1. Introduction

Rechargeable metallic lithium batteries have attracted great attentions to industrial community in recent years due to the promising future of solid-state batteries,[1–3] lithium–sulfur,[4] and lithium–air[5] batteries. The obstacles of the application for metallic lithium anodes include at least five factors: 1) inhomogeneous deposition and dissolution of lithium; 2) side reactions between lithium and liquid electrolyte during storage and electrochemical reactions; 3) large volume variation of electrodes; 4) low melting temperature of metallic lithium; 5) soft and sticky properties. The inhomogeneous stripping and plating of lithium will lead to the uneven volume variation, which will result in the fresh lithium exposing into and reacting with the electrolyte, eventually leading to the failure of the cell. Li *et al.*[5] have studied the effect of electrochemical deposition/dissolution order and found that the problem of non-uniform Li-ion plating/stripping during charge/discharge is very serious. In order to improve the electrochemical performance and safety property, numerous strategies such as tuning the electrolytes and salts,[6–15] searching the additives,[16–21] treating the separators,[22,23] using the lithium alloy anodes,[24] using ceramic/polymer solid electrolytes,[25,26] and coating buffer layers[27–36] have been proposed. Coating methods have been considered as one of the most direct and effective strategies among them. The coating precursors can be solid, liquid and gas. Recently Wen[28] grew an $Li_3N$ coating layer on the lithium anode through an *in-situ* gas reaction method, exhibiting excellent performance. Since the gas is pervasive and can fully react with lithium in all the active sites, thus a dense and uniform buffer layer can be obtained by gas reaction method. Therefore, gas reaction method is regarded as simple and producible, which is suitable for large scale application in energy storage field.

Herein, four kinds of gases include Ar, $CO_2$–$O_2$ (2:1), $N_2$, and $CO_2$–$O_2$–$N_2$ (2:1:3) were used to react with metallic lithium anode and their effects on electrode performance were studied. Hereafter, three different coating layers on lithium tablets were obtained, which may mainly contain $Li_2CO_3$, $Li_3N$,[28] and the mixture of $Li_3N$ and $Li_2CO_3$ respectively. The SIMS data shows the coating layer on lithium tablets have different density and uniformity. The micro conductive performance of the four as-prepared lithium tablets was analyzed by SPM. Li/Li symmetrical cells were assembled to study the stripping/plating performance. In addition, the SEM and SIMS characterizations before/after cycle in Li/S cell were compared. The electrochemical testing results indicate that a SEI-like composition formed on the lithium tablets can modulate the interfacial stabilization between the lithium foil and the ether electrolyte.

## 2. Experiment

### 2.1. Electrodes preparation

The lithium tape was polished by the polishing sticks, and after that it was placed on the punched copper foil and rolled

*Project supported by the National Key Research and Development Program of China (Grant No. 2016YFB0100100), the National Natural Science Foundation of China (Grants Nos. 52315206 and 51502334), and the Fund from Beijing Municipal Science & Technology Commission, China (Grants No. D171100005517001).

†Corresponding author. E-mail: hli@iphy.ac.cn

© 2017 Chinese Physical Society and IOP Publishing Ltd 

together to get the copper-clad lithium tape. The copper-clad lithium tape was punched into small lithium tablets with a diameter of 14 mm. Then lithium tablets were put into 4 homemade gas treatment devices under the flowing of Ar, $N_2$, $CO_2$–$O_2$ (2:1), and $CO_2$–$O_2$–$N_2$ (2:1:3) for five minutes, respectively (The numbers in the brackets are the flow ratios of the gases). After that, the devices filled with each kind of gases were put into the oven at 60 °C for at least 1 hour. The treated lithium metals were used as the anodes.

The S cathode was prepared via a solid phase synthesis method through the following procedures: a certain amount of sulfide and ketjen black carbon were mixed with a strict stoichiometric ratio (mass ratio = 1 : 1) and ground uniformly in the mortar. The blended powder was collected and transferred into a glass tube, heating in a muffle furnace at 3 °C/min till 155 °C and was kept for 24 h. The obtained powder was mixed with PVDF in a 10:1 mass ratio and stirred with moderate NMP to make a well-distributed slurry. The slurry was coated on Al foil with 100-μm valid thickness. The coated Al foil was dried in a vacuum oven at 60 °C for 6 h and punched into tablets with a diameter of 14 mm.

### 2.2. Electrochemical measurement

The CR2032 coin cells were assembled with a crimping machine (MSK-110, MTI, China) in an argon gas filled glove box ($H_2O$ and $O_2 < 0.1$ ppm, Braun UNILAB). 1-M ether electrolyte with DOL : DME = 1 : 1 (volume ratio) was adopted in both Li/Li symmetrical cell and Li/S cell. The electrochemical performance of lithium cells was measured at room temperature by Land BA2100A Battery Test System (Wuhan, China). The current density and capacity density for the measurement of the symmetrical cell were 1 mA/cm$^2$ and 1 mAh/cm$^2$ respectively. The current for the measurement of Li/S cell was 100 μA, corresponding to 0.5 C rate and a current density of 65 μA/cm$^2$. The voltage range was set from 1.5 V to 3 V. After one cycle, the Li/S cell was disassembled in the glove box with the disassemble machine (MSK-110, MTI, China). The lithium tablets were washed at least three times with DME. And then the lithium tablets were dried in vacuum box for at least 4 hours. Finally, the lithium tablets were analyzed by various characterization instruments.

### 2.3. Characterization

The XRD pattern of the four kinds of gas treated lithium tablet was acquired from the x-ray diffract meter (Bruker D8 Advance, China).

To acquire the surface micro conductivity distribution, a new characterization method was developed: First the sample was pasted on a small iron tablet (thickness: 0.5 mm, diameter: 15 mm) with conductive copper glue. And then the prepared sample was put on the sample stage of Scanning Probe Microscope (Multimode8, Bruker, China) to measure the current distribution at nano-scale in PF-TUNA mode. The scanning area was around micrometer and the resolution of the current was about 0.1 fA.

In order to get the element depth profile from the surface into the inner layer, SIMS workstation (Hiden Analytical, England) was used to collect the chemical information across depth of the sample. The resolution and sensitivity are 1 ppm and 1 Å respectively.

The morphologies of surface and cross-section were analyzed by using the SEM (HITACHI S4800).

Considering the air contamination, all measurements and transfer processes were conducted under an inert atmosphere or in vacuum environment.

## 3. Results and discussion

Figure 1 shows the XRD pattern of the four kinds of gases treated lithium tablets. It can be seen that under different gases, three peaks centered at 36.173°, 52.086°, and 65.186° are mainly appeared, which all belong to the reflection peaks of metallic lithium. However, the Ar and $CO_2$–$O_2$ (2:1) treated samples only show peaks at 36.173° and 65.186° while the $N_2$ and $CO_2$–$O_2$–$N_2$ (2:1:3) treated samples show all of the peaks, regardless the slight different of peak intensity. It is assumed that the different treatments may change the arrangement of lithium atoms, resulting in various prefer orientations. In spite of this, there is no new peak appearing in the reflections, which is possible due to that the coating layers are too thin to be detected by the XRD.

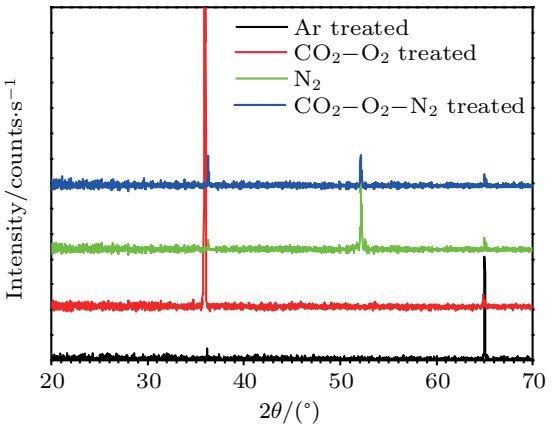



**Fig. 1.** (color online) XRD of lithium tablets treated by argon (black line), $CO_2$–$O_2$ (2:1) (red line), $N_2$ (green line), and $CO_2$–$O_2$–$N_2$ (2:1:3) (blue line) gases respectively.

In order to identify the existence of nitrogen in the coating layers, SIMS was applied as it is capable of detecting elements in a high resolution. Figure 2 shows the SIMS spectra of the treated lithium tablets. From the spectra, it can be seen that nitrogen and oxygen do exist in all of the samples,

which is probably because the difficult of removing all the $N_2$ in the Glove box. In addition, because of the high reaction activity, the lithium will react with residual $N_2$ or $O_2$ in the instruments during the transfer and fabrication process. Figure 2(a) shows the Ar-treated sample has a relative thick interlayer. Figure 2(b) shows a sharpest interface and thinnest interlayer, which reveals the $CO_2$–$O_2$ (2:1)-treated sample shows a thinner coating layer because of the good passivation effect of the $Li_2CO_3$. The $N_2$-treated sample has a wider nitrogen distribution, which indicates the coverage of $Li_3N$ on the lithium tablet is non-uniform. The $CO_2$–$O_2$–$N_2$ (2:1:3) treated sample shows a sharper interface than the $N_2$ treated one, which manifests the dense and even film has been formed on the lithium tablet.

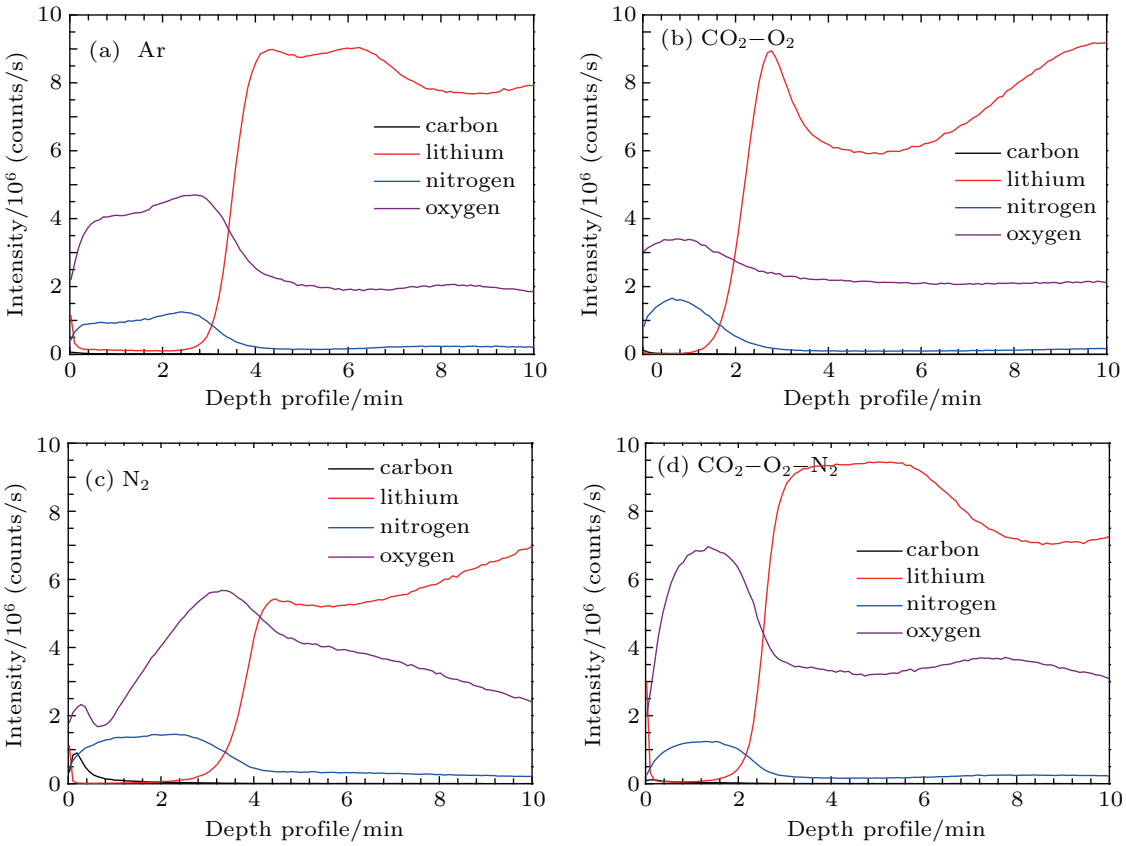



**Fig. 2.** (color online) SIMS of lithium tablets treated by argon (a), $CO_2$–$O_2$ (2:1) (b), $N_2$ (c), and $CO_2$–$O_2$–$N_2$ (2:1:3) (d) gases respectively.

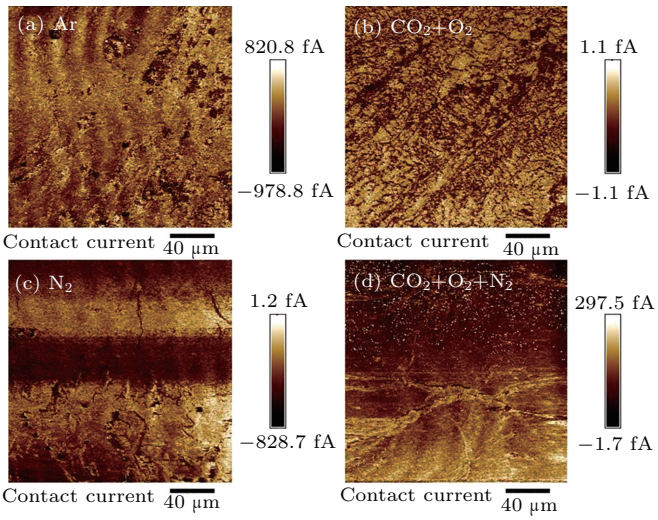



**Fig. 3.** (color online) Current distribution (obtained by SPM) of lithium tablets treated by argon (a), $CO_2$–$O_2$ (2:1) (b), $N_2$ (c), and $CO_2$–$O_2$–$N_2$ (2:1:3) (d) gases respectively.

The SPM was used to evaluate the density and uniformity of the formed layer on the lithium tablets. From the PF-TUNA mapping (Fig. 3), it can be observed that the Ar treated lithium tablet has a relative uniform and high micro-current distribution. The $CO_2$–$O_2$ (2:1)-treated sample reveals even current distribution, which may be due to the uniformly formed $Li_2CO_3$ coating layer on the lithium tablets. The $N_2$-treated sample shows an uneven current distribution, indicating the non-uniformity of $Li_3N$ on the lithium tablet. And the $CO_2$–$O_2$–$N_2$ (2:1:3)-treated sample shows a moderate current distribution between the treatment situations by $N_2$ and $CO_2$–$O_2$ (2:1).

To further analyze the current distribution and the property of different gases treated lithium tablets, NanoScope Analysis software (1.80 (Build R1.126200), Copyright©2016 Bruker Corporation) is used to count the current in the scanning area. A data process of shifting the minimum value of the current to zero is used to get the following histogram

(Fig. 4). Figure 4 displays that the micro-currents of the $CO_2$–$O_2$ (2:1), $N_2$, and $CO_2$–$O_2$–$N_2$ (2:1:3)-treated lithium metal anode significantly reduce than the Ar-treated one. The $CO_2$–$O_2$ (2:1)-treated lithium tablet shows the smallest average current, which indicates the $Li_2CO_3$ layer may forms on the lithium surface and has a high resistance. This infers that the layer is very dense or thick, preventing the lithium tablet from the electron contact with the current collector. The current of $N_2$-treated lithium tablet only slightly shifts to the low current region, which means the $Li_3N$ is film is no denser than $Li_2CO_3$. The $CO_2$–$O_2$–$N_2$ (2:1:3)-coated sample shows a moderate current distribution between the $CO_2$–$O_2$ (2:1) and $N_2$-treated sample, which implying that the mixture gases may react with lithium tablet and $Li_2CO_3$ and $Li_3N$ compounds are formed on the surface, leading to a middle current distribution.

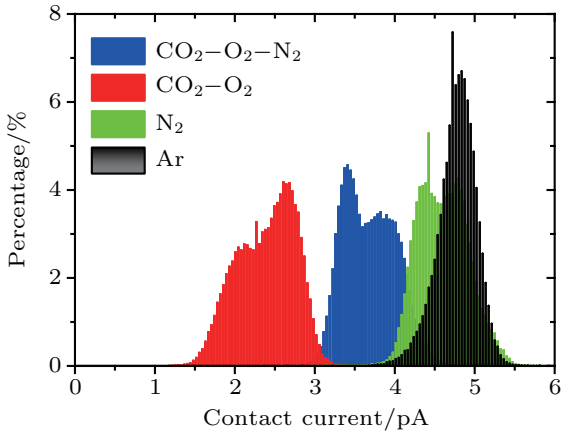



**Fig. 4.** (color online) Current histogram of lithium tablets treated by argon (black line), $CO_2$–$O_2$ (2:1) (red line), $N_2$ (green line), and $CO_2$–$O_2$-$N_2$ (2:1:3) (blue line) gases respectively.

Figure 5 shows the performance of Li/Li symmetrical cell with gas treatment. The cell with Ar-treated sample shows a very large polarization (over 100 mV), which reveals unstable electrochemical stability. The cell with $CO_2$–$O_2$ (2:1)-treated lithium tablet shows a much higher stability and smaller polarization than those of the Ar-treated sample, but still higher than the other two cases. The $N_2$-treated sample shows a small polarization, but it is not as stable as the condition in $CO_2$–$O_2$ (2:1) treatment. Among them, the cell with $CO_2$–$O_2$–$N_2$-(2:1:3)-treated lithium tablet possesses both the relative small polarization as well as high stability. Considering lithium will continuously react with $N_2$ to result in uneven reaction sites, $N_2$-treated lithium tablet could not be well protected. The $Li_2CO_3$ is relative more dense and stable than $Li_3N$, but the cell with lithium tablet coated by $Li_2CO_3$ has a bigger polarization which is not preferred in the batteries. Hence, the $CO_2$–$O_2$–$N_2$ (2:1) treatment process is more applicable in real cell systems.

Figure 6 shows the electrochemical properties of Li/S cell with different gases treated lithium tablets. The $CO_2$–$O_2$–$N_2$ (2:1:3)-treated sample shows the best capacity retention and the most stable Coulombic efficiency according to Figs. 6(b) and 6(c). Figure 6(a) shows $CO_2$–$O_2$ (2:1)-treated sample has a large overcharge. It is assumed that the dense $Li_2CO_3$ has a large resistance and poly-sulfides will accumulate near the surface on the lithium tablet. Moreover, the $Li_2CO_3$ component is not stable with poly-sulfides. However, the $Li_3N$ buffer layer can block the shuttle of the poly-sulfides effectively. Thus the $CO_2$–$O_2$–$N_2$ (2:1:3)-treated sample combines the advantages of both $Li_2CO_3$ and $Li_3N$ coating layers and shows better performance.

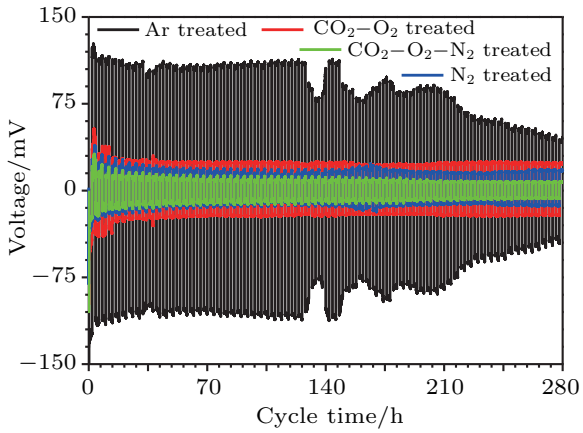



**Fig. 5.** (color online) Electrochemical performances of lithium symmetrical cell with lithium tablets treated by argon (black line), $CO_2$–$O_2$ (2:1) (red line), $N_2$ (green line), and $CO_2$–$O_2$–$N_2$ (2:1:3) (blue line) gases respectively.

Figure 7 shows the morphology evolution of the gas protected lithium before and after cycling. No obvious difference could be observed among the un-cycled samples, indicating the morphology does not change largely and the passivated film is very thin. However, these 4 kinds of lithium metal anodes exhibit different surface morphology evolutions after electrochemical striping and plating in Li/S cells. In Ar-treated lithium anode, lots of cracks appear, and the similar morphology evolution was observed from $CO_2$–$O_2$ (2:1)- and $N_2$-treated lithium anodes. It is also displayed that $CO_2$–$O_2$ (2:1)-treated sample has a number of clusters of cracks and holes, while $N_2$-treated samples only has isolated holes. As expected, the $CO_2$–$O_2$–$N_2$ (2:1:3)-treated anode inherits the surface morphology features from the $CO_2$–$O_2$ (2:1) and the $N_2$ treated sample, which shows both cracks and isolated holes. If $N_2$ gas contributes to the $Li_3N$ formation and the $CO_2$–$O_2$ (2:1) gas provides a denser and more uniform passivated $Li_2CO_3$ film, thus the $CO_2$–$O_2$–$N_2$ (2:1:3)-treated sample possesses the merits from both the $CO_2$–$O_2$ (2:1) and $N_2$ treating methods. As is well known, $Li_2CO_3$ has a lower electronic and ionic conductivity compared to that of $Li_3N$, as a result, the $CO_2$–$O_2$–$N_2$ (2:1:3)-treated sample has a dense, uniform, and ionic passable protection layer. It is also in consistent with the electrochemical cycling performance and XRD data.

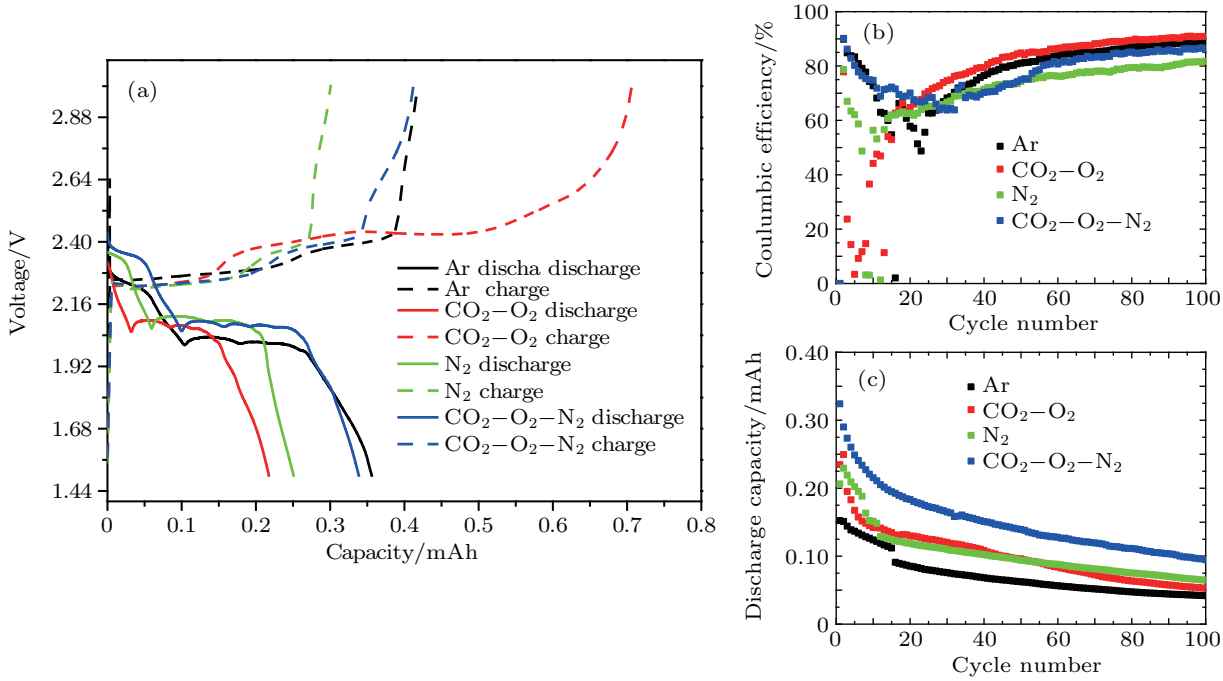



**Fig. 6.** (color online) Electrochemical performances of Li/S cell with lithium tablets treated by argon (black line), $CO_2$–$O_2$ (2:1) (red line), $N_2$ (green line), and $CO_2$–$O_2$–$N_2$ (2:1:3) (blue line) gases respectively. (a) The 1st cycle curve; (b) the Coulombic efficiency; (c) the discharge capacity.

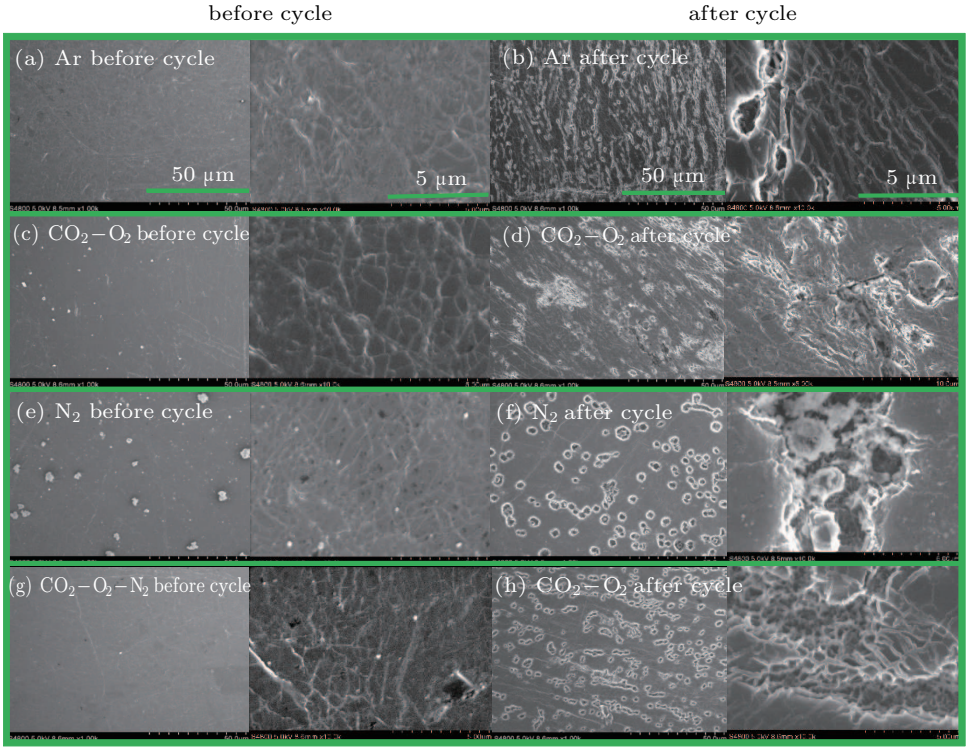



**Fig. 7.** (color online) Morphology evolution before (a), (c), (e), (g), and after (b), (d), (f), (h) cycle of Li/S cell with lithium tablets treated by argon [(a) and (b)], $CO_2$–$O_2$ (2:1) [(c) and (d)], $N_2$ [(e) and (f)], and $CO_2$–$O_2$–$N_2$ (2:1:3) [(g) and (h)] gases respectively.

As is known that F is the main element in the SEI composition. The redox of polysulfide on the lithium anode is the main reason of poor property. In order to further identify the protection effect of the gas treatment, we analyzed the F and S element distributions on the three protected samples after cycling (Fig. 8). Figure 8(a) shows the $CO_2$–$O_2$ (2:1) treated sample contains more F after one cycle. The $N_2$ treated sample shows the lowest F amounts. The small peak of red curve in Figure 8(b) shows that S was accumulated in the inner layer of the $CO_2$–$O_2$ (2:1)-treated sample, which is consistent with the poor cycle performance. The $CO_2$–$O_2$–$N_2$ (2:1:3)-treated sample shows the lowest S content especially in the inner-layer. It means there is little poly-sulfides decomposed on the $CO_2$–$O_2$–$N_2$ (2:1:3)-treated sample.

Considering the lithium surface process, the possible chemical reaction equations among lithium, $N_2$, $O_2$, and $CO_2$ are given as follows: $6Li+N_2 \rightarrow 2Li_3N$; $Li+2CO_2+2O_2 \rightarrow 2Li_2CO_3$; $4Li+O_2 \rightarrow 2Li_2O$. According to the Gibbs energy variation, we can obtain the $\Delta G$ of each reaction equations. They are $-308.3$ kJ/mol, $-1475.27$ kJ/mol, $-374$ kJ/mol respectively, which means the $Li_2CO_3$ is easier to nucleate on the lithium surface than $Li_3N$. Besides, the existence of $N_2$ decreases the collision probability among the lithium atom, $CO_2$ and $O_2$ molecules, and also helps to form $Li_3N$ simultaneously. The competition reaction mechanism finally makes the formation of mixed $Li_2CO_3$ and $Li_3N$ component film on the lithium tablet.

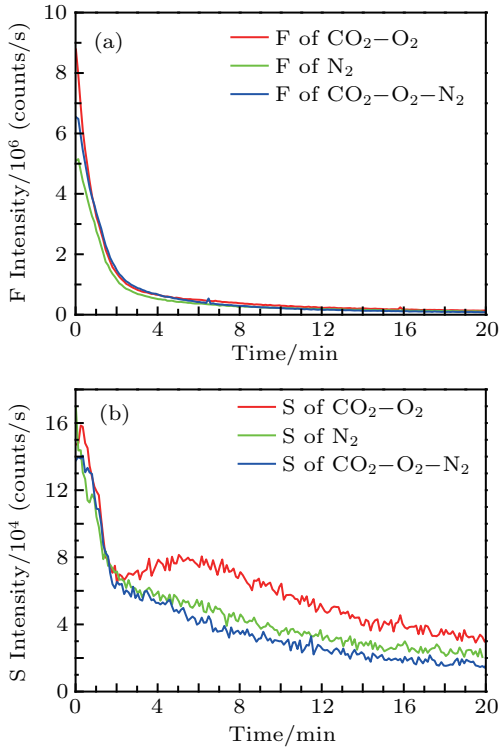



**Fig. 8.** (color online) SIMS depth profile of lithium tablets treated by $CO_2$–$O_2$ (2:1) (red line), $N_2$ (green line), and $CO_2$–$O_2$–$N_2$ (2:1:3) (blue line) gases respectively. (a) F depth profile after cycle; (b) S depth profile after cycle.

## 4. Conclusion and perspectives

In summary, we successfully fabricated three kinds of gases treated coating layers on lithium metal tablet: $Li_3N$, $Li_2CO_3$, and mixed buffer layer. The coated buffer layers effectively improve the storage and cycling stability of the lithium metal anode. The mixed buffer layer with $Li_3N$ and $Li_2CO_3$ combines the advantages of both components and shows the best stability and lowest polarization in Li/S cell system. The reaction between Li and $N_2$ is uneven, and the coverage of $Li_3N$ buffer layer is not so uniform. With the help of $Li_2CO_3$, a denser and more stable buffer layer is formed. The mixed buffer layer has relative high ion conductivity compared with pure $Li_2CO_3$ buffer layer. The SEM and SIMS together prove mixed buffer layer has a higher stability than the single component buffer layer during the cycling.

The developed gas protected electrode demonstrates good property and also allows the large scalable production in reality. We believe with the further purification of lithium surface and optimization of gas treatment process, metallic lithium will make further step towards the practical application in lithium batteries.

## References


[1] Yao X Y, Huang B X, Yin J Y, Peng G, Huang Z, Gao C, Liu D and Xu X X 2016 *Chin. Phys. B* **25** 018802
[2] Li H 2017 *Nat. Sci. Rev.* **4** 106
[3] Li H and Xu X X 2016 *Energ. Storg. Sci. Tech.* **5** 607 (in Chinese)
[4] Yin Y X, Yao H R and Guo Y G 2016 *Chin. Phys. B* **25** 018801
[5] Bruce P G, Freunberger S A, Hardwick L J and Tarascon J M 2012 *Nat. Mater.* **11** 19
[6] Li W, Zheng H, Chu G, Luo F, Zheng J, Xiao D, Li X, Gu L, Li H, Wei X, Chen Q and Chen L 2014 *Faraday Discuss.* **176** 109
[7] Ding F, Xu W, Chen X, Zhang J, Engelhard M H, Zhang Y, Johnson B R, Crum J V, Blake T A, Liu X and Zhang J G 2013 *J. Electrochem. Soc.* **160** A1894
[8] Suo L, Hu Y S, Li H, Armand M and Chen L 2013 *Nat. Commun.* **4** 1481
[9] Walker W, Giordani V, Uddin J, Bryantsev V S, Chase G V and Addison D 2013 *J. Am. Chem. Soc.* **135** 2076
[10] Liu Z, Chai J, Xu G, Wang Q and Cui G 2015 *Coord. Chem. Rev.* **292** 56
[11] Zu C, Azimi N, Zhang Z and Manthiram A 2015 *J. Mater. Chem. A* **3** 14864
[12] Liu P, Ma Q, Fang Z, Ma J, Hu Y S, Zhou Z B, Li H, Huang X J and Chen L Q 2016 *Chin. Phys. B* **25** 078203
[13] Miao R, Yang J, Xu Z, Wang J, Nuli Y and Sun L 2016 *Sci. Rep.* **6** 21771
[14] Zhang S, Li W J, Ling S G, Li H, Zhou Z B and Chen L Q 2015 *Chin. Phys. B* **24** 078201
[15] Zhao C Z, Cheng X B, Zhang R, Peng H J, Huang J Q, Ran R, Huang Z H, Wei F and Zhang Q 2016 *Energy Storage Materials* **3** 77
[16] Zu C X and Manthiram A 2014 *Journal of Physical Chemistry Letters* **5** 2522
[17] Li W, Yao H, Yan K, Zheng G, Liang Z, Chiang Y M and Cui Y 2015 *Nat. Commun.* **6** 7436
[18] Lu Y, Tu Z, Shu J and Archer L A 2015 *J. Power Sources* **279** 413
[19] Xu W T, Peng H J, Huang J Q, Zhao C Z, Cheng X B and Zhang Q 2015 *ChemSusChem* **8** 2892
[20] Choudhury S and Archer L A 2016 *Adv. Electron. Mater.* **2** 1500246
[21] Zhang X Q, Cheng X B, Chen X, Yan C and Zhang Q 2017 *Adv. Funct. Mater.* **27** 1605989
[22] Wu J Y, Lin S G, Yang Q, Li H, Xu X X and Chen L Q 2016 *Chin. Phys. B* **25** 078204
[23] Liu K, Zhuo D, Lee H W, Liu W, Lin D, Lu Y and Cui Y 2016 *Adv. Mater.* **29**
[24] Chen C, Yang Y F and Shao H X 2014 *Electrochim. Acta* **137** 476
[25] Stone G M, Mullin S A, Teran A A, Hallinan D T, Minor A M, Hexemer A and Balsara N P 2012 *J. Electrochem. Soc.* **159** A222
[26] Lu Y, Tu Z and Archer L A 2014 *Nat. Mater.* **13** 961
[27] Huang J, Peng J Y, Ling S G, Yang Q, Qiu J L, Lu J Z, Zheng J Y, Li Hong and Chen L Q 2017 *Chin. Phys. B* **26** 068201
[28] Ma G, Wen Z, Wu M, Shen C, Wang Q, Jin J and Wu X 2014 *Chem. Commun.* **50** 14209
[29] Zheng G, Lee S W, Liang Z, Lee H W, Yan K, Yao H, Wang H, Li W, Chu S and Cui Y 2014 *Nat. Nanotechnol.* **9** 618
[30] Kazyak E, Wood K N and Dasgupta N P 2015 *Chem. Mater.* **27** 6457
[31] Kozen A C, Lin C F, Pearse A J, Schroeder M A, Han X, Hu L, Lee S B, Rubloff G W and Noked M 2015 *ACS Nano* **9** 5884
[32] Liu Q C, Xu J J, Yuan S, Chang Z W, Xu D, Yin Y B, Li L, Zhong H X, Jiang Y S, Yan J M and Zhang X B 2015 *Adv. Mater.* **27** 5241
[33] Cheng X B Zhang Q 2015 *J. Mater. Chem. A* **3** 7207
[34] Han X G, Gong Y H, Fu K, He X F, Hitz G T, Dai J Q, Pearse A, Liu B Y, Wang H, Rubloff G, Mo Y F, Thangadurai V, Wachsman E D and Hu L 2016 *Nat. Mater.* **16** 572
[35] Li N W, Yin Y X, Yang C P and Guo Y G 2016 *Adv. Mater.* **28** 1853
[36] Zheng G, Wang C, Pei A, Lopez J, Shi F, Chen Z, Sendek A D, Lee H W, Lu Z, Schneider H, Safont-Sempere M M, Chu S, Bao Z and Cui Y 2016 *ACS Energy Lett.* **1** 1247